

Plasma photonic crystal

Wei LI (✉)¹, Yong ZHAO¹, Ruizhen CUI², Haitao ZHANG²

¹ Department of Automation, Tsinghua University, Beijing 100084, China

² Department of Precision Instruments, Tsinghua University, Beijing 100084, China

© Higher Education Press and Springer-Verlag 2009

Abstract Plasma photonic crystals are presented in this paper. A plasma photonic crystal can control the propagation of electromagnetic waves. Similar to other photonic crystals, the permittivity of a plasma photonic crystal is distributed as periodic arrays. The properties of periodic arrays of plasma can broaden the range of frequency and enhance the efficiency of beam-wave interaction. In special uses, the behavior of plasma shows that it has properties of photonic crystals.

Keywords plasma photonic crystal, dispersion relation, band gap, permittivity

1 Introduction

The use of background plasma in a backward wave oscillator (BWO) or traveling wave tube (TWT) can increase the space charge limiting current by a factor $(1 - n_i/n_e)^{-1}$, where n_i/n_e is the number density of the background plasma normalized to the number density in the electron beam, and enhance the efficiency of microwave devices. Many theories have been employed to explain the efficiency enhancement [1–19]. In this paper, plasma filled in the microwave device has been regarded as plasma photonic crystals [20].

In recent years, great interest has been aroused on photonic crystals, and an increasing number of new photonic crystals have been studied and fabricated. The ability to confine and control light would have important implications for quantum optics and other devices: plasma in microwave devices can modify the dispersive properties and enhance the efficiency of the interaction [1–7] among the plasma lens [8], the plasma antenna [9,10], and the plasma stealth [10]. All these reveal that plasma can control the light (electromagnetic wave). Photonic crystals, the optical analogues of electronic crystals, provide a way

to achieve the goal, i.e., to confine or control the light. Combinations of electrons and ions can be used to obtain the required three-dimensional periodic variations in dielectric constants. In some cases, plasma can be used as photonic crystals, namely plasma photonic crystals. Three-dimensional photonic crystals fabricated in low-loss plasma show only a weak stop band, i.e., a range of frequencies at which propagation of light is forbidden, at the wavelengths of interest. In this paper we provide the concept of plasma photonic crystal. It shows a large stop band and a strong attenuation of light within this band.

Section 2 offers the concept of the plasma photonic crystal. In Sect. 3, the theory of electromagnetic wave propagation in plasma photonic crystals is presented, while Sect. 4 gives a conclusion.

2 Concept of plasma photonic crystals

Plasma is a very complicated material which is the fourth state of matter. It is composed of electrons and ions. Botton and Ron [11,12] have investigated that under strong wave modulation, plasma injected into the interaction region forms a periodical distribution of the plasma density called density grating and exerts a periodic perturbation on the dielectric constant. The grating induces distributed feedback (DFB), which in turn influences wave propagation and the interaction between the wave and the electron beam. In the dielectric Cerenkov maser, a corrugate waveguide loaded with the plasma (shown in Fig. 1) is studied. The standing wave field in the cavity is formed by the slow waves. The neutral plasma injected into the interaction region is influenced by two counter propagating waves R and S along the $\pm z$ direction, and the total electric field can be written as

$$E(r,z) = R(r,z)\exp(-jk_0z) + S(r,z)\exp(jk_0z), \quad (1)$$

where $R(r,z)$ is the forward wave, $S(r,z)$ is the backward wave, and k_0 is the wave number of the space harmonic for TM mode.

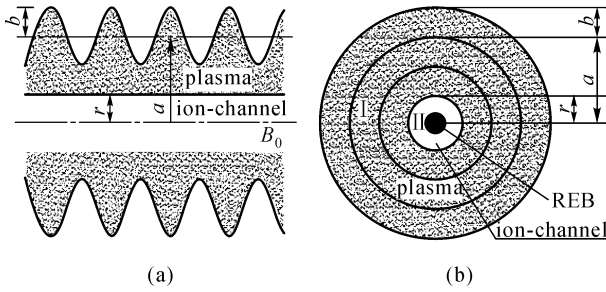


Fig. 1 Schematic figure of corrugate waveguide filled with plasma. (a) Cutaway view; (b) section diagram

As shown by Botton [11], the waves modulate the plasma density through the ponderomotive potential that induces a self-consistent potential. The self-consistent potential directly contributes to density grating formation, and the plasma density can be expressed as

$$n_e = n_0 \exp[-g_0 \cos(2k_0 z)], \quad (2)$$

where n_0 is the unperturbed plasma density; k_0 is the wave number; g_0 is the modulation parameter:

$$g_0 = \frac{e^2}{4m_e \omega^2 k T_e} \frac{\tau}{1 + \tau} |R| \cdot |S|,$$

$\tau = T_e/T_i$ is the electron to ion temperature ratio, $|R|$ and $|S|$ are the absolute values of the forward wave and backward wave respectively, T_e and T_i are the electron and ion temperatures respectively, ω is the frequency of plasma, k is the Boltzmann constant; the rest mass and charge of the electron are denoted by m_e and e , respectively.

Once the density grating is formed, the corrugate waveguide can be regarded as one filled with a dielectric having a periodically varying dielectric constant. The plasma dielectric constant can be obtained as

$$\varepsilon = 1 - \frac{\omega_p^2}{\omega^2} \exp[-g_0 \cos(2k_z z)], \quad (3)$$

where k_z is the Boltzmann constant in the z direction; $\omega_p = \sqrt{e^2 n_0 / (m_e \varepsilon_0)}$ is the plasma frequency, in which the rest mass and charge of electron are denoted by m_e and e respectively, and ε_0 is the dielectric constant of the non-magnetized plasma. The space period of the dielectric constant $L = \pi/k_z$ can be obtained. Figures 2 and 3 show the periodic distribution of plasma density and the permittivity in the z direction, respectively. The properties of the plasma periodic distributions show that the plasma can be treated as photonic crystals called plasma photonic crystals.

To obtain the propagation properties of the electronic wave controlled by the plasma photonic crystal, the permittivity which distributes periodically is described approximately as a rectangle distribution in Fig. 3. The

grating distributed in the axial direction can be approximately replaced by a series of dielectric blocks of thickness δ and space period L . δ is determined by half thickness of the actual grid in any period (shown in Fig. 3).

$$\delta = \frac{|\pi - \arccos[-\ln(\cosh g_0)/g_0]|}{k_z}. \quad (4)$$

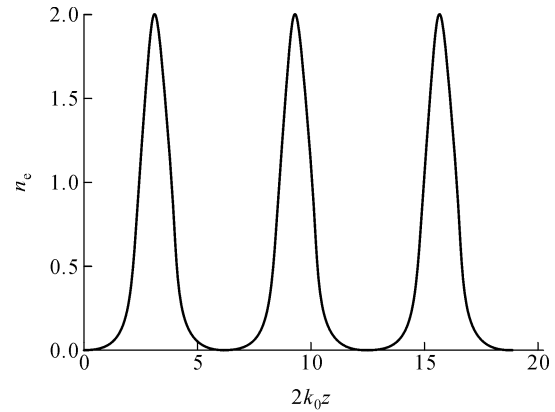


Fig. 2 Periodic distribution of plasma density along z direction

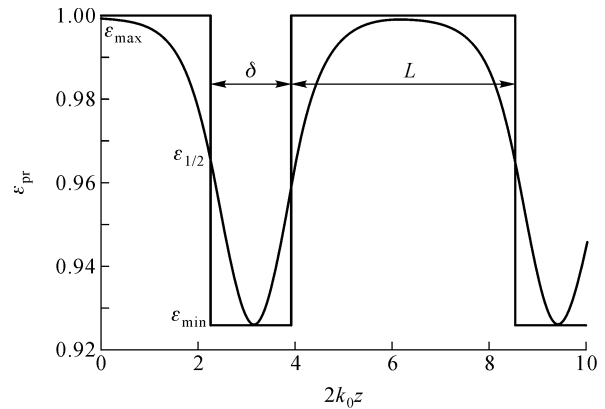


Fig. 3 Dielectric function of plasma density grating and its equivalent model ($\omega_p/\omega = 0.01$, $g_0 = 2$)

The characteristic of the permittivity is then equivalent as a uniformity anisotropic medium, i.e., properties of the periodicity medium are equivalent as a uniformity anisotropic medium in the z direction and r direction, the θ direction does not need to be sought in case of cornerwise symmetry, and relative permittivity can be expressed as follows [14]:

$$\begin{aligned} \varepsilon_r &= 1 + \left(\frac{\varepsilon_0}{\varepsilon} - 1\right) \frac{\delta}{L} \\ &= 1 - (1 - \varepsilon_p) \frac{|\pi - \arccos[-\ln(\cosh g_0)/g_0]|}{\pi}, \end{aligned} \quad (5)$$

$$\begin{aligned}\varepsilon_z &= \frac{1}{1 - \left(1 - \frac{\varepsilon_0}{\varepsilon}\right) \frac{\delta}{L}} \\ &= \frac{1}{1 - \left(1 - \frac{1}{\varepsilon_p}\right) \frac{|\pi - \arccos[-\ln(\cosh g_0)/g_0]|}{\pi}},\end{aligned}\quad (6)$$

$$\vec{\varepsilon} = \varepsilon_0 \begin{bmatrix} \varepsilon_r & 0 & 0 \\ 0 & 1 & 0 \\ 0 & 0 & \varepsilon_z \end{bmatrix}, \quad (7)$$

where ε_p is the dielectric constant of the magnetized plasma and $\vec{\varepsilon}$ is the tensor of the dielectric constant of plasma.

This allows derivation of the equivalent uniformity anisotropic medium permittivity of the plasma immersed in a finite magnetic field \mathbf{B}_0 as the following expression:

$$\vec{\varepsilon} = \varepsilon_0 \begin{bmatrix} \varepsilon_1 & -\varepsilon_2 & 0 \\ \varepsilon_2 & \varepsilon_1 & 0 \\ 0 & 0 & \varepsilon_3 \end{bmatrix}, \quad (8)$$

where

$$\varepsilon_1 = 1 - \frac{\xi^2(1-j\chi)}{(1-j\chi)^2 - \tau^2},$$

$$\varepsilon_2 = \frac{j\tau\xi^2}{(1-j\chi)^2 - \tau^2},$$

$$\varepsilon_3 = 1 - \frac{\xi^2}{1-j\chi},$$

$$\tau = \frac{\omega_c}{\omega}, \chi = \frac{\gamma_{\text{eff}}}{\omega}, \xi = \frac{\omega_p}{\omega}.$$

$\omega_p = [n_e e^2 / (m_e \varepsilon_0)]^{1/2}$ is plasma frequency, $\omega_c = eB_0/m_e$ ($\mathbf{B}_0 = B_0 \vec{e}_z$, B_0 is the intensity of magnetic field) is electron cyclotron frequency, γ_{eff} is electron efficiency collision frequency, j is unit imaginary number, and ω is electromagnetic wave cornerwise frequency.

3 Theory of electromagnetic wave propagation in plasma photonic crystals

Figure 1 shows the studied model, where the inside wall of the slow wave structure is assumed as an ideal conductor and cosine variety. The inside radius of the waveguide can be expressed as $R(z) = a + b \cos(k_0 z)$, where a is average radius of the waveguide, b is the depth of the ripple, $k_0 = 2\pi/z_0$ is the wave number of the corrugation, z_0 is the

periodic length of the ripple, and r_i is the radius of the ion-channel. A relative electron-beam (REB) is injected into the waveguide along the axes and forms an ion-channel [3,4].

Assuming that the plasma is confined within the slow wave region, the plasma density is $n(z)$ and the longitudinal electric field satisfies the active wave equation. In the case of steady state, assuming the time parameter is $e^{j\omega t}$, the following results are obtained from Refs. [5,6]:

a) When the magnetic field is infinite ($B_0 \rightarrow \infty$) and the ion-channel is omitted ($r_i \rightarrow 0$) from the TM modes, the dispersion equation is [3–6]

$$\det[(F_{0,1})_{n,s}] = 0, \quad (9)$$

where

$$(F_{0,1})_{n,s} = \left[1 + (n-s) \frac{k_{z,n} k_0}{k^2 - k_{z,n}^2} \right] C_{ns1}^J,$$

k_z is the wave number of the z direction, $k_{z,n}$ is wave number of the n rank harmonic, and

$$C_{ns1}^J = \sum_{q=0}^{\infty} \frac{(p_1 b)^{2q+|n-s|} J_0^{2q+|n-s|} p_1 a}{2^{2q+|n-s|} q! (q+|n-s|)!},$$

in which q , n and s are integrals respectively.

For the TE modes, the dispersion equation is [3–6]

$$\det[(G_{0,2})_{n,s}] = 0, \quad (10)$$

where

$$(G_{0,2})_{n,s} = \frac{(k^2 - k_z^2)^2 \omega_p^2}{[(k^2 - k_z^2)^2 - 1] \omega^2} \left[\frac{k_z \sqrt{1 - \omega_p^2/\omega^2}}{\sqrt{k^2 - k_z^2}} S_{ns2}^N + (n-s) \frac{k_0}{\sqrt{k^2 - k_z^2} \sqrt{1 - \omega_p^2/\omega^2}} T_{ns2}^N \right],$$

$$T_{ns2}^N = \sum_{q=1}^{\infty} \frac{(p_2 b)^{2q+|n-s|} N_0^{2q+|n-s|-1} p_2 a}{2^{2q+|n-s|} q! (q+|n-s|)!},$$

$$S_{ns2}^N = \sum_{q=0}^{\infty} \frac{(p_2 b)^{2q+|n-s|} N_0^{2q+|n-s|+1} p_2 a}{2^{2q+|n-s|} q! (q+|n-s|)!}.$$

J_0 and N_0 are the zero-order Bessel and Neumann functions, respectively.

b) When the magnetic field is zero ($B_0 = 0$) and the ion-channel is omitted ($r_i \rightarrow 0$) from the TM modes, the dispersion equations are

$$\det[(F_{0,1})_{n,s}] = 0, \quad (11)$$

$$(F_{0,1})_{n,s} = \left[1 + (n-s) \frac{k_{z,n} k_0}{(1 - \omega_p^2/\omega^2) k^2 - k_{z,n}^2} \right] C_{ns1}^J. \quad (12)$$

For the TE modes, the dispersion equations are

$$\det[(G_{0,2})_{n,s}] = 0, \tag{13}$$

$$(G_{0,2})_{n,s} = \left[-\frac{K^2(K^2 + k_z^2 - k^2)(\omega^2 - \omega_p^2)}{(-1 + K^4)\omega^2 - K^4\omega_p^2} \right] \times \left[\frac{k_{z,n}}{K} S_{ns}^N + (n-s)\frac{k_0}{K} T_{ns}^N \right], \tag{14}$$

where $K^2 = \gamma^2 + k^2\varepsilon$ and $\gamma = jk_z$.

Through complex calculations, the following results and dispersion curves are obtained by using Eqs. (9)–(14).

The dispersion curves of the magnetic field are infinite and shown in Fig. 4, where the plasma density is $n_p = 2 \times 10^{11} \text{ cm}^{-3}$, the voltage is $V = 400 \text{ kV}$, the current is $I = 1 \text{ kA}$, the spatial periodic length of the ripple is $z_0 = 1.67 \text{ cm}$, the average radius of the waveguide is $a = 1.445 \text{ cm}$ and the ripple depth is $b = 0.145 \text{ cm}$. Most parameters of Fig. 5 are the same as Fig. 4, except in Fig. 5 the plasma density is $n_p = 4 \times 10^{11} \text{ cm}^{-3}$. When the magnetic field is zero, the dispersion curves are shown in Fig. 6, the parameters are the same as Fig. 5 except for the magnetic field. In Figs. 4–6, 1 and 3 are the TM_{01} spatial harmony waves, and 2 and 4 are the TE_{01} spatial harmony waves. $\omega = kc$ and $\omega = k_z v$ denote the curve of the velocity of light and the spatial charge waves, respectively.

Considering Figs. 4–6, Fig. 4 shows that the TM_{01} mode work frequency range is 8–10 GHz, and the TE_{01} is about 12.5 GHz. Comparing Fig. 4 to Fig. 5 we can establish that with the plasma density increasing, TM_{01} mode frequency will have a 1 GHz ascending shift, but the TE_{01} ascending shift is small. For high level modes, the influence of the plasma density is smaller, the TM_{01} mode dispersion curves have no significant changes. However, the TE_{01} mode dispersion curves have an ascending shift when the magnetic field is zero. There are clearly passage bands and

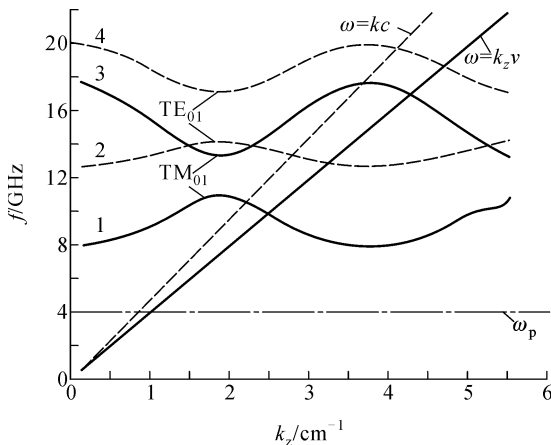


Fig. 4 Dispersion curves of magnetic field are infinite ($a = 14.45 \text{ mm}$, $b = 1.45 \text{ mm}$, $z_0 = 16.7 \text{ mm}$ and $n_p = 2 \times 10^{11} \text{ cm}^{-3}$)

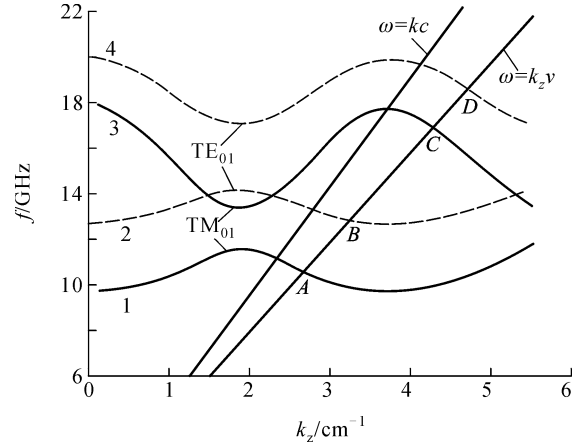


Fig. 5 Dispersion curves of magnetic field are infinite ($n_p = 4 \times 10^{11} \text{ cm}^{-3}$, $B_0 \rightarrow \infty$)

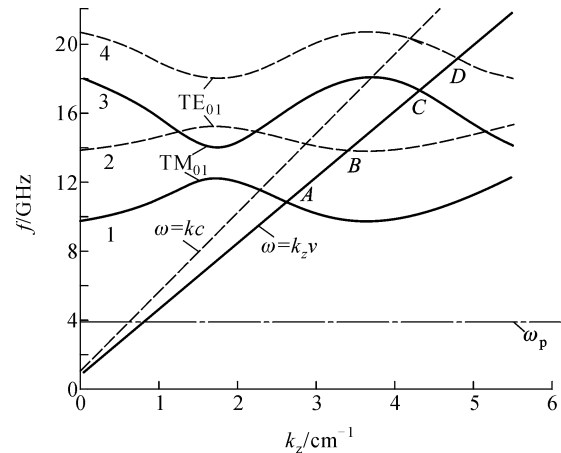


Fig. 6 Dispersion curves of magnetic field are zero ($n_p = 4 \times 10^{11} \text{ cm}^{-3}$)

forbidden bands, an indication that plasma density grating is a kind of photonic crystal. Plasma photonic crystals can control the electromagnetic wave, reflect the electromagnetic wave at some frequency range and induce other frequency waves passing through. When the plasma photonic crystals are injected into the microwave devices, the frequency and the conversion efficiency are significantly increased [11–13]. By adjusting the magnetic field and changing the plasma parameters such as plasma density, we are able to control the electromagnetic waves.

4 Conclusion

The permittivity of plasma photonic crystals is periodically distributed and can control electromagnetic waves similar to other photonic crystals. The permittivity of plasma photonic crystals can be changed from 10 to an imaginary number. The theory of this special photonic crystal is interesting and requires further research.

Acknowledgements This work was supported by the National Natural Science Foundation of China (Grant No. 10475048) and the China Postdoctoral Fund (Grant No. 023201005). The authors would like to thank Prof. Zhao Dazun of Beijing Institute of Technology and Prof. Ye Weimin of National University of Defense Technology for valuable discussions.

References

1. Yablonovich E. Inhibited spontaneous emission in solid-state physics and electronics. *Physical Review Letters*, 1987, 58(20): 2059–2062
2. John S. Strong localization of photons in certain disordered dielectric superlattices. *Physical Review Letters*, 1987, 58(23): 2486–2489
3. Liu S G, Barker R J, Zhu D J, et al. Basic theoretical formulations of plasma microwave electronics, Part I: A fluid model analysis of electron beam-wave interactions. *IEEE Transactions on Plasma Science*, 2000, 28(6): 2135–2151
4. Liu S G, Barker R J, Yan Y, et al. Basic theoretical formulations of plasma microwave electronics, Part II: Kinetic theory of electron beam-wave interactions. *IEEE Transactions on Plasma Science*, 2000, 28(6): 2152–2165
5. Li W, Wei Y Y, Xie H Q, et al. “Cold” dispersion relation of corrugated waveguide filled with plasma immersed in a finite magnetic field. *Chinese Physics*, 2003, 12(5): 532–537
6. Li W, Gong M L, Wei Y Y, et al. The dispersive properties of a dielectric-rod loaded waveguide immersed in a magnetized annular plasma. *Chinese Physics*, 2004, 13(1): 54–59
7. Li W, Gao H, Gong M L, et al. Theory of electromagnetic wave propagation in a plasma-filled corrugate waveguide immersed in a finite magnetized field. *Chinese Physics*, 2004, 13(8): 1296–1301
8. Goncharov A A, Zatuagan A V, Protsenko I M. Focusing and control of multiaperture ion beams by plasma lenses. *IEEE Transactions on Plasma Science*, 1993, 21(5): 578–581
9. Dwyer T, Greig J, Murphy D, et al. On the feasibility of using an atmospheric discharge plasma as an RF Antenna. *IEEE Transactions on Antennas and propagation*, 1984, 32(2): 141–146
10. Chaudhury B, Chaturvedi S. Three-dimensional computation of reduction in radar cross section using plasma shielding. *IEEE Transactions on Plasma Science*, 2005, 33(6): 2027–2034
11. Botton M, Ron A. Self-induced distributed feedback in plasma-filled Cherenkov free electron masers. *Physics of Fluids*, 1992, B4(7): 1979–1988
12. Botton M, Ron A. Efficiency enhancement of a plasma-filled backward-wave oscillator by self-induced distributed feedback. *Physical Review Letters*, 1999, 66(19): 2468–2471
13. Lin A T, Chen L. Plasma-induced efficiency enhancement in a backward wave oscillator. *Physical Review Letters*, 1989, 63(26): 2808–2811
14. Xiao S, Mo Y L. Study of open cavity filled with plasma density grating. *IEEE Transactions on Plasma Science*, 1999, 27(5): 1495–1500
15. Kosai H, Garate E P, Fisher A. Plasma-filled dielectric Cherenkov maser. *IEEE Transactions on Plasma Science*, 1990, 18(6): 1002–1007
16. Carmel Y, Minami K, Kehs R A, et al. Demonstration of efficiency enhancement in a high-power backward-wave oscillator by plasma injection. *Physical Review Letters*, 1989, 62(20): 2389–2392
17. Carmel Y, Minami K, Lou W, et al. High-power microwave generation by excitation of a plasma-filled rippled boundary resonator. *IEEE Transactions on Plasma Science*, 1990, 18(3): 497–506
18. Lin A T. Magnetic field effects on plasma-filled backward wave oscillators. *Proceedings of SPIE*, 1991, 1407: 234–241
19. Ali M M, Minami K, Ogura K, et al. Absolute instability for enhanced radiation from a high-power plasma-filled backward-wave oscillator. *Physical Review Letters*, 1990, 65(13): 855–858
20. Li W, Zhan H T, Gong M L. Plasma photonics crystal. *Optical Technique*, 2004, 30(3): 263–266 (in Chinese)